High-Frequency Guided Waves for Corrosion Thickness Loss Monitoring

Daniel Chew[1], Bernard Masserey[2], Paul Fromme[1]

[1] Department of Mechanical Engineering, University College London, UK
[2] Department of Mechanical Engineering, HES-SO University of Applied Sciences and Arts Western Switzerland, Fribourg, Switzerland

p.fromme@ucl.ac.uk

Abstract. Adverse environmental conditions result in corrosion during the life cycle of marine structures such as pipelines, offshore oil platforms, and ships. Generalized corrosion leading to wall thickness loss can cause the degradation of the integrity, strength, and load bearing capacity of the structure. Nondestructive detection and monitoring of corrosion damage in difficult to access areas can be achieved using high frequency guided waves propagating along the structure. Using standard ultrasonic wedge transducers with single sided access to the structure, specific high frequency guided wave modes (overlap of both fundamental Lamb wave modes) were generated that penetrate through the complete thickness of the structure. The wave propagation and interference of the guided wave modes depend on the thickness of the structure and were measured using a noncontact laser interferometer. Numerical simulations using a 2D Finite Element model were performed to visualize and predict the guided wave propagation and energy transfer across the plate thickness. During laboratory experiments the wall thickness was reduced uniformly by milling of one steel plate specimen. In a second step, wall thickness reduction was induced using accelerated corrosion for two mild steel plates. The corrosion damage was monitored based on the effect on the wave propagation and interference (beating effect) of the Lamb wave modes in the frequency domain. Good agreement of the measured beatlengths with theoretical predictions was achieved and the sensitivity of the methodology ascertained, showing that high frequency guided waves have the potential for corrosion damage monitoring at critical and difficult to access locations.

Keywords: Corrosion Detection, Guided Ultrasonic Waves, Wall Thickness Loss, Lamb Waves

1. Introduction

Corrosion leading to wall thickness loss is an important problem for pipelines and partially submerged marine structures, e.g., ships and offshore platforms [1]. Generalized corrosion prevalent in ship hulls leads to thickness reduction, limiting their remaining service life [2]. Nondestructive measurements can help to quantify and monitor corrosion severity, with ultrasonic measurements having good sensitivity to small wall thickness losses [3]. Ship hulls, offshore oil platforms and oil storage tanks are built using large plate components which can be efficiently monitored using guided ultrasonic wave array systems [4], as guided ultrasonic waves (GUW) can propagate over large distances in thin structures [1, 5]. Guided wave structural health monitoring (SHM) systems usually operate at low frequencies below the cut-off frequencies for higher order wave modes to selectively generate only the fundamental (A_0 or S_0) wave modes, simplifying signal interpretation [6, 7]. Image fusion, combining both fundamental modes with selective, tuned excitation has been shown to improve defect localization [8] The dispersive nature makes guided waves sensitive to thickness reduction, which has been employed for corrosion detection [9, 10], e.g. using the A_0 mode at constant group velocity [11].

However, low operating frequency range corresponds to long wavelengths and thus limited sensitivity for the detection of small defects. The application of guided ultrasonic wave modes in the higher frequency-thickness range has been investigated to obtain better sensitivity for wall thickness loss [12]. This allows for the nondestructive inspection of structures over reasonably long distances and can be employed even if local access to the inspected part is limited [13]. Depending on the chosen frequency-thickness operating point, wavelengths are comparable to those commonly used in bulk wave ultrasonic testing (e.g. M-Skip [14]), possibly allowing good sensitivity for the detection of small defects [15]. The S_0 mode (around 5 MHz mm) was used for corrosion detection in aircraft structures [16], and longitudinal modes (above 15 MHz mm) were employed for plate inspection [15]. Higher order mode clusters of guided wave modes up to about 20 MHz mm were used to monitor plates [17]. Systematic comparison of different guided wave modes and choice of operating point (frequency-thickness product) was conducted [13]. Good results were found for the A_1 Lamb mode, SH_1 shear horizontal mode and lower frequency guided waves, depending on the specific inspection problem.

High frequency guided waves (superposition of the first anti-symmetric A_0 and symmetric S_0 Lamb wave modes) at around 6-7 MHz mm have been employed for fatigue crack monitoring [18]. These high frequency guided wave modes in plates are easily generated and received selectively above the cut-off frequencies of the higher Lamb wave modes using standard Rayleigh wave angle beam transducers. The interference between the two fundamental modes and the resulting beating effect was employed for the inspection of ribbed structures [19]. The resulting beatlength is very sensitive to the frequency-thickness product. This was visualized using 2D Finite Element (FE) simulations to predict the wave propagation phenomena at approximately 5 MHz mm frequency thickness product and was investigated to monitor the thickness reduction due to generalized corrosion in steel specimens [20, 21]. The concept was in a first step demonstrated by monitoring the thickness reduction for milled, uniform thickness

specimens to develop reference measurements and gain an understanding of the accuracy of the methodology. During accelerated corrosion of steel plate specimens, the thickness reduction was monitored using longitudinal and high frequency guided ultrasonic waves to verify the applicability for thicknesses reduction quantification.

2. 2D Finite Element Simulations

The propagation of the superposition of the two fundamental Lamb modes in a mild steel plate (Young's modulus 200 GPa, Poisson's ratio 0.29, density 7900 kg/m^3) was predicted using a two-dimensional (2D) explicit Finite Element (FE) model in the commercial software ABAQUS. The cross-section with length 600 mm and thickness ranging from 9 mm to 11 mm (in 0.1 mm steps) was meshed with four-node plane strain elements (CPE4R) using a Cartesian grid. As a general rule, a minimum of 10 nodes per wavelength is required in order to reduce the numerical dispersion to an acceptable level [22]. For high-frequency guided waves, the mode shapes have to be approximated accurately and finer spatial sampling is required [23]. A uniform grid size of 100 μm was selected, corresponding to approximately 60 nodes per wavelength (Rayleigh wavelength 5.8 mm at 0.5 MHz). The time step was set at 10 ns to fulfill the stability criteria, with 0.2 ms overall simulation time for the wave to completely propagate along the plate length. Rayleigh damping (β = 0.5 ns) was applied to approximate the reduction in wave amplitude observed experimentally (combination of dissipation and beam spreading). The selected excitation signal was a sinusoidal, 10-cycle tone burst (sinusoid in a Hanning window) at a center frequency of 0.5 MHz (bandwidth 0.4-0.6 MHz). The fundamental modes A_0 and S_0 were excited by generating a Rayleigh wave at one end of the plate. The mode shapes of the Rayleigh wave at the center frequency were modulated with the excitation signal, adding a phase shift of $\pi/2$ between in-plane and out-of-plane displacement components [24]. The resulting displacement time series were imposed at each node on a vertical line through the plate thickness until the end of excitation duration. The out-of-plane displacement signals were recorded at monitoring points (every 1 mm) on the top (excitation) surface with a sampling time step of 100 ns. For one plate thickness (9 mm) the full wavefield (von Mises stress) was saved at different time steps and the time signals were recorded at the top and bottom of the plate.

3. High-Frequency Guided Wave Interference

In the frequency range of interest for this investigation (around 5 MHz mm), there is a slight difference between the phase velocities of the first anti-symmetric (A_0) and symmetric (S_0) Lamb wave modes and they have not fully converged towards a Rayleigh wave (Fig. 1). Both modes have very similar mode shapes and stress profiles close to the plate surfaces, either symmetric or anti-symmetric on the two plate sides. During wave propagation there is a continual shift in relative phase, causing the transfer of the wave energy through the plate thickness.

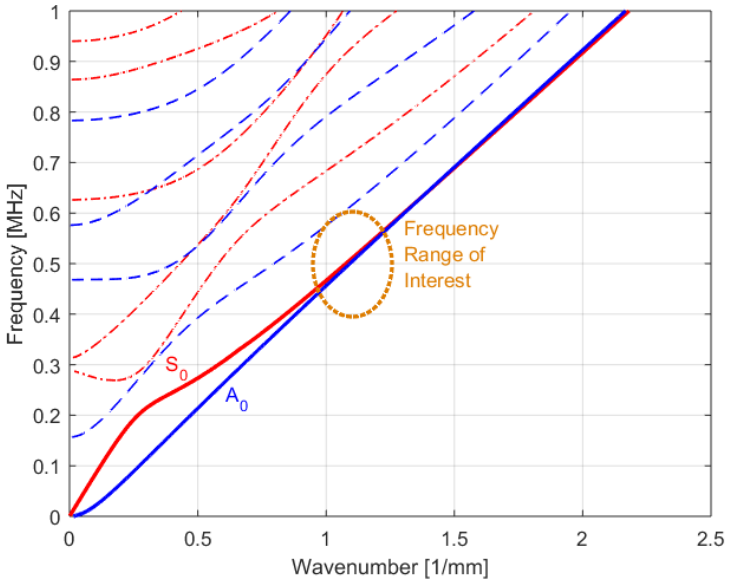

Figure 1. Dispersion diagram for 10 mm thick mild steel plate; frequency range of interest around 0.5 MHz marked, overlap of A_0 and S_0 guided wave modes.

The significant distance for this energy exchange, the so-called beatlength [25] or beat wavelength [26], is given by

$$L = \frac{2\pi}{k_{A0} - k_{S0}}, \tag{1}$$

with k_{A0} and k_{S0} the wavenumbers of the A_0 and S_0 mode, respectively. This interference depends on the frequency thickness product, as it is governed by the inverse of the difference between the wave numbers of the two fundamental Lamb wave modes, and is thus very sensitive to small thickness reduction.

The 2D FE model was employed to visualize the wave propagation along a 9 mm thick steel plate. The wave excitation was prescribed to simulate a transducer placed on the top surface at the left end of the plate (A_0 and S_0 modes in phase on the upper surface). For the different time snapshots shown in Fig. 2, it can be observed that as the wave pulse propagates along the plate, the distribution of the wave field (von Mises stress) through the thickness changes. The initial snapshot (20 μs) shows most of the wave pulse energy located in the upper half of the plate thickness. Gradually more energy is transferred to the lower half of the plate thickness (30 μs), with reduced amplitude on the top surface and increased amplitude on the bottom surface (40 μs). As the wave propagates farther, energy is transferred back to the upper half of the plate (50 and 60 μs), with increased amplitude on the top surface (70 μs). The time snapshots at 40 and 70 μs show that on the plate surface with lower amplitude the signal appears as two shorter pulses. This can be attributed to the slightly different group velocities of the two wave modes and the frequency dependence of the beating as the wave pulse contains frequencies around the center frequency of 0.5 MHz. It should be noted that simulations were conducted for free plate boundaries, not considering fluid loading which would attenuate the signals and lead to an additional drop in amplitude with propagation distance. As both fundamental modes have very similar modeshape profiles close to the plate surface, both modes would be subject to similar attenuation and the beating effect would not be significantly affected.

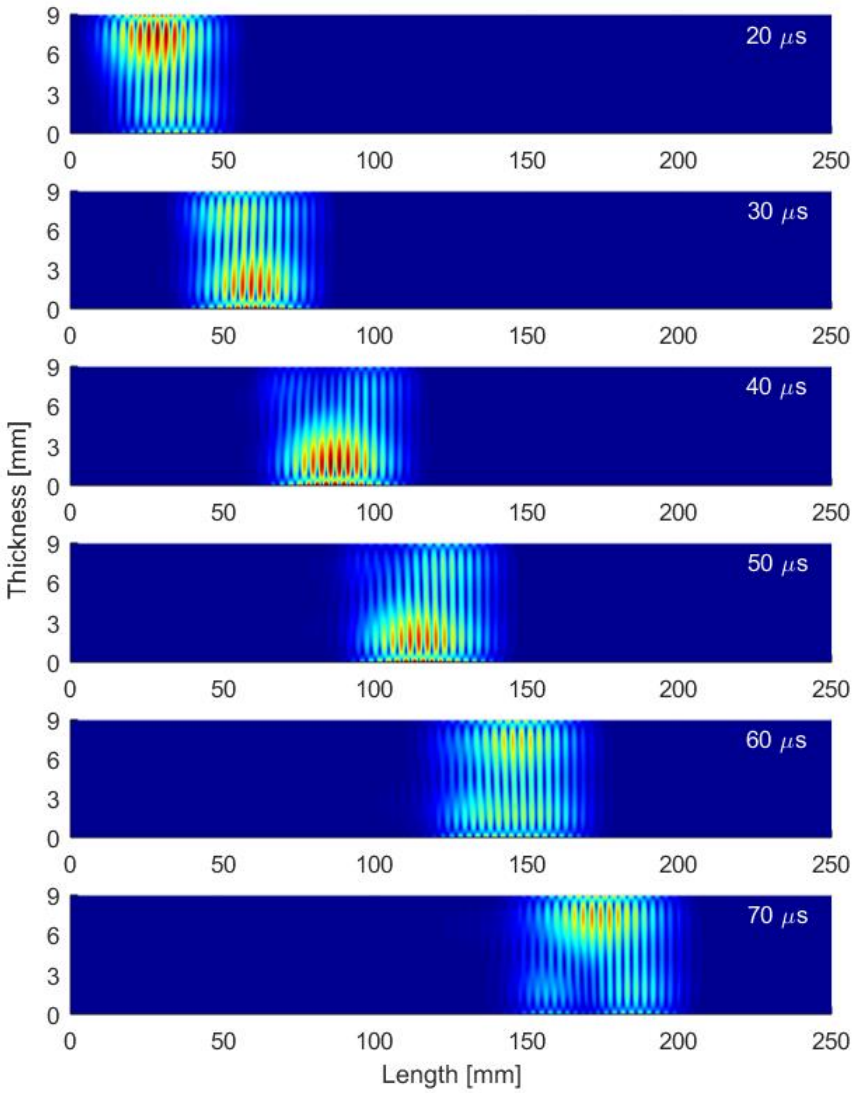

Figure 2. FE simulation of wave propagation along 2D plate specimen (von Mises stress) at different time steps; excitation frequency 0.5 MHz; 10 cycles; 9 mm thick steel plate.

The corresponding time traces (out-of-plane displacement) on the top and bottom surface of the 9 mm thick model are shown in Fig. 3. On the top surface (left column) the reduction in amplitude to about 90 mm propagation distance can be observed, followed by an increase in amplitude of the time signal up to 180 mm propagation distance. This is matched on the bottom surface by an increase in amplitude of the recorded time signals to 90 mm, followed by a reduction to 180 mm propagation distance. At points with low amplitude (top: 90 mm; bottom: 180 mm) time signals with two shorter pulses matching observations from Fig. 2 can be seen.

Time signals were evaluated in the frequency domain for 450 mm propagation distance to avoid overlap with reflections from the plate end (length: 600 mm). Using Matlab, the signal magnitude was extracted at a frequency of 0.45 MHz for each monitoring point using Fast Fourier Transform (FFT). For the employed 10-cycle excitation signal, the signal amplitude at 0.45 MHz is approximately half of the maximum amplitude at 0.5 MHz. An evaluation frequency slightly below the center excitation frequency of 0.5 MHz was employed to achieve shorter beatlengths with multiple amplitude minima occurring over the monitoring distance of 450 mm.

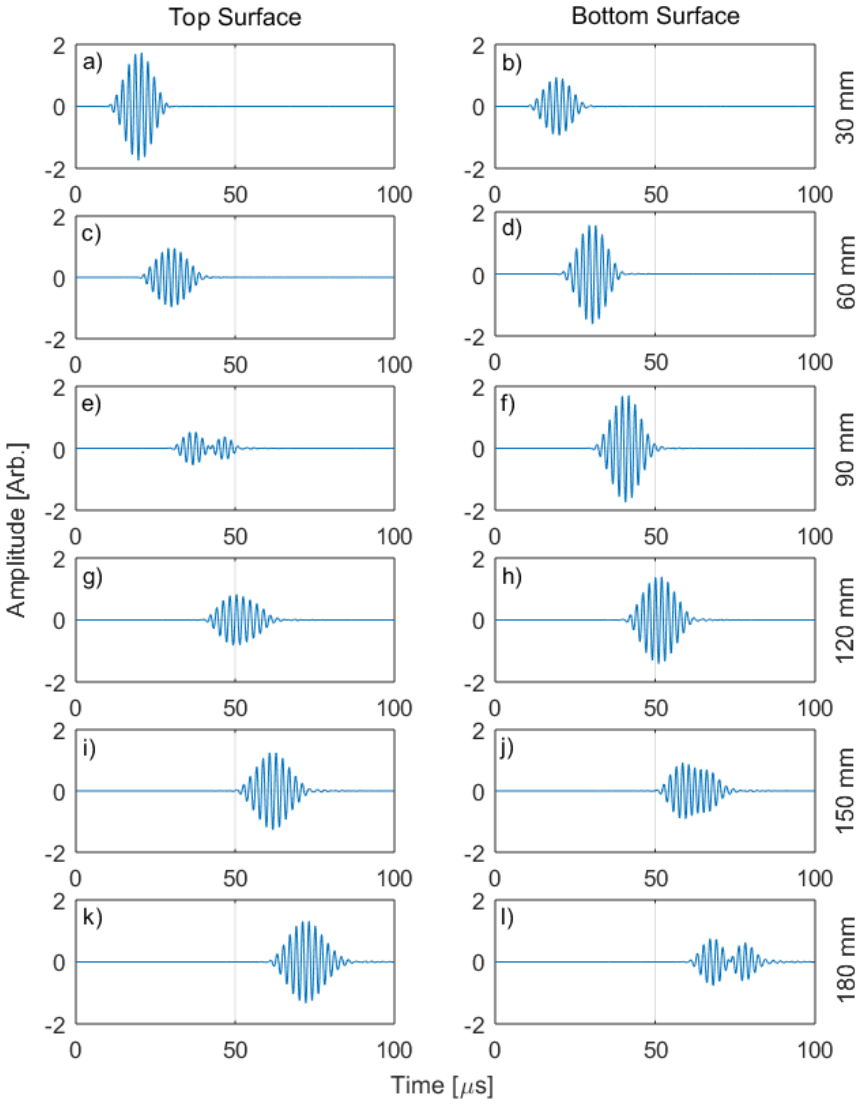

Figure 3. FE simulation of wave propagation along 2D plate specimen, displacement (out-of-plane) time traces at different locations, top and bottom surface; excitation frequency 0.5 MHz; 10 cycles; 9 mm thick steel plate.

The corresponding amplitude curves along the propagation distance are shown in Fig. 4 for four different plate thicknesses. The characteristic pattern due to the constructive and destructive interference between the two fundamental Lamb wave modes with a reduction in amplitude and subsequent increase can be clearly observed. For the 11 mm thick plate (Fig. 4a) the amplitude reduces almost to zero at 155 mm and then increases again to a maximum at 305 mm before decreasing again. With decreasing plate thickness, the length scale of this characteristic pattern decreases, and for a 9 mm thick plate (Fig. 4d), minima at 70, 205, 340 mm and maxima at 135, 270, 405 mm can be observed. This corresponds to a larger difference in the wavenumbers of the A_0 and S_0 modes for lower frequency-thickness products (Fig. 1) leading to a shorter beatlength. It has to be noted that this effect depends strongly on the frequency-thickness product, so that in the time domain the amplitude reduction is less pronounced as the wave pulse contains energy over a range of frequencies.

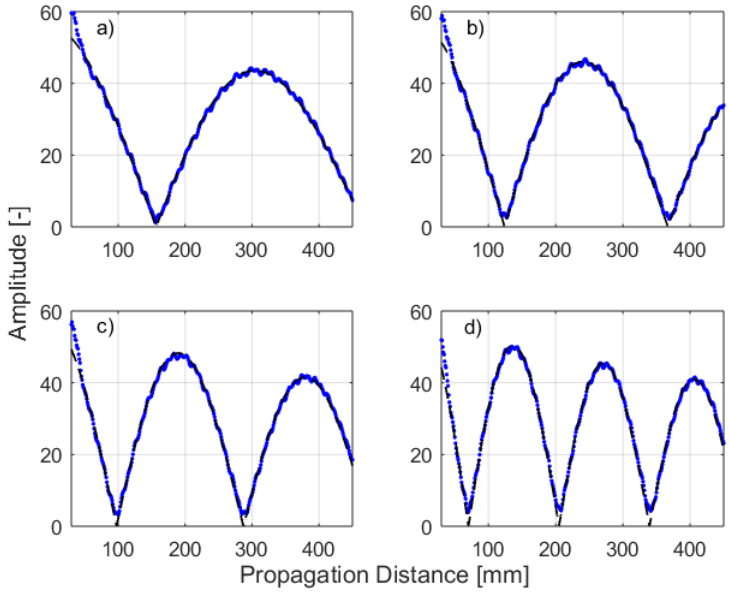

Figure 4. FE simulation of amplitude of high frequency guided wave at 0.45 MHz (FFT) along uniform steel specimen: (a) 11.0 mm; (b) 10.4 mm; (c) 9.8 mm, (d) 9.0 mm thickness; simulation amplitude: blue dots; exponential fit: black solid line.

To evaluate this, the amplitude curve at 0.45 MHz was fitted in Matlab with the expected behavior (exponential decrease due to applied Rayleigh damping, absolute of cosine for beatlength, initial amplitude and phase) to extract the beatlength for each plate thickness simulation. Good agreement of the fitted amplitude curve to the simulation results can be seen in Fig. 4, with some minor variations of the extracted amplitude values due to additional higher wave modes present in the signal and minor numerical inaccuracies. Previous evaluations for the experimental data at 0.5 MHz had shown slight variations due to the fitting procedure of the observed amplitude values with limited propagation length relative to the beatlength (e.g. fit of curve with only one minimum and maximum for the thicker plate, Fig. 4a).

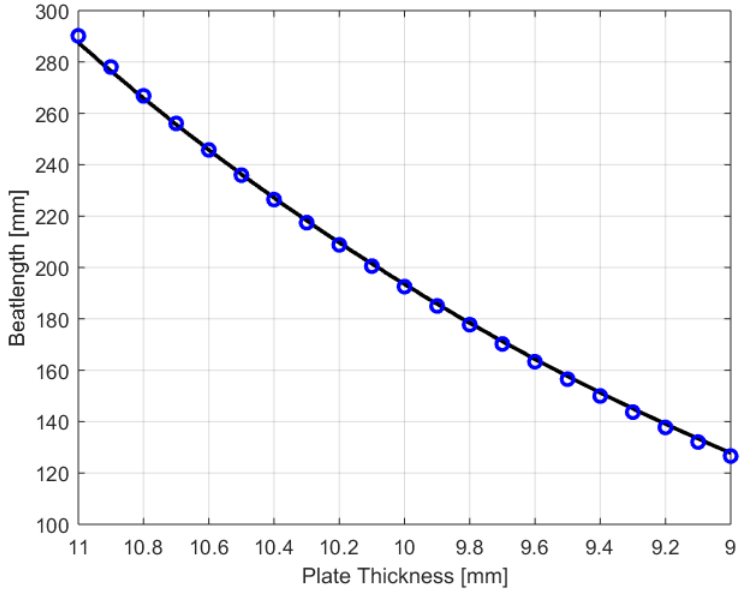

Figure 5. Comparison of beatlength evaluated at 0.45 MHz (FFT) from FE simulation along uniform steel specimen: blue dots; with theoretical prediction (Disperse): black solid line.

Simulations and evaluations were conducted for each plate thickness between 9 and 11 mm (in steps of 0.1 mm). The resulting beatlength values are shown in Fig. 5. Theoretical beatlengths were predicted based on the difference between the wavenumbers of the fundamental modes (Fig. 1, Eq. 1) calculated using Disperse [27]. This shows the expected good agreement with a maximum difference of 1% between the simulation evaluation and theory. It can be seen that the beatlength is very sensitive to changes in the plate thickness, e.g., a predicted reduction in the beatlength by more than 50% for a change of plate thickness by 2 mm (< 20%).

4. Experiments

Three plate specimens (650 mm x 100 mm) were cut from a single plate of mild steel (EN3B – AISI 1020) and milled to 11 mm thickness in order to correct a slight curvature in the original plate material. This mild steel is similar in mechanical properties to that of steel used in shipbuilding (Poisson's ratio 0.29, yield strength 295 MPa, tensile strength 395 MPa, Young's modulus 200 GPa and density 7900 kg/m^3). One specimen was milled down in approximately 0.2 mm steps to a final thickness of 9.43 mm to achieve a uniform thickness reduction. The thickness was measured after each milling step using a digital micrometer and was found to be uniform within +/- 0.01 mm.

The wall thickness of two of the mild steel specimens was reduced by accelerated corrosion, using the reverse of impressed current cathodic protection [1]. The setup consisted of a DC voltage source, with the steel plate partially submerged as the anode in NaCl solution (salt water), suspended above a copper plate cathode at the bottom of the tank (Fig. 6). The DC voltage source supplied a current of approximately 5A at 12V. Due to increased corrosion rates at the plate edges, the corrosion was monitored using standard through thickness longitudinal pulse-echo ultrasonic measurements (5 MHz center frequency) at 12 evenly spaced locations along the plate center line. The thickness values from the bulk ultrasonic measurements were averaged and taken as the actual thickness for comparison to the guided wave measurements. As expected, variability of measured thickness along the specimen length increased with increasing corrosion thickness loss up to a maximum variation of approximately 0.3 mm, with the standard deviation of measurements below 0.1 mm for all cases.

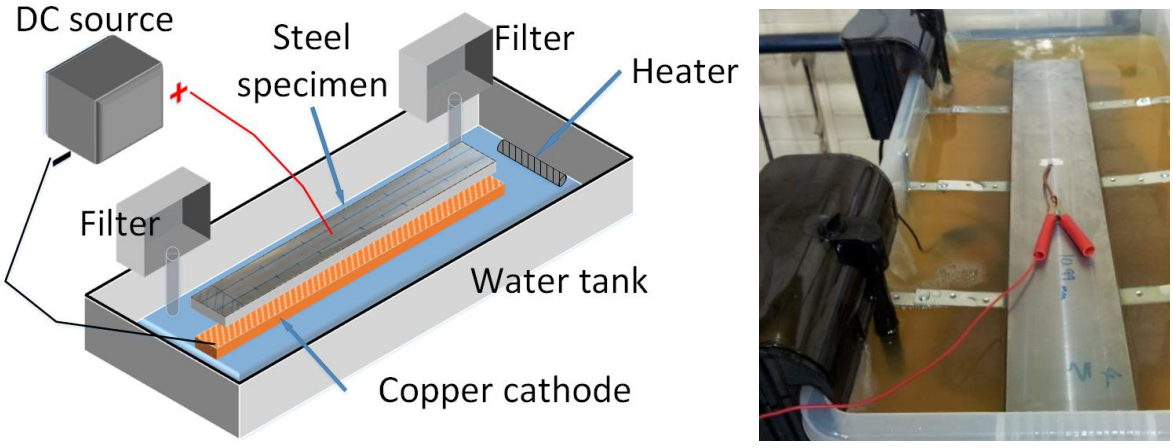

Figure 6. Accelerated corrosion setup impressing DC current on steel plate specimen in NaCl solution, with the steel specimen and copper cathode connected to DC source, water tank with filters and heater; left: schematic; right: photograph.

Based on the measured corrosion rates, the accelerated corrosion process was interrupted approximately every 30 hours to conduct the guided wave measurements for thickness reductions matching approximately the 0.2 mm milling steps. The average thickness was in general close to the required thickness and reduced from 11.0 mm to 9.42 mm (specimen #A), respectively 9.84 mm (specimen #B), for the two corroded specimens. Fluctuations in the achieved corrosion rate occurred due to changes in the temperature and the amounts of corrosion products causing varying conductivity of the NaCl solution. Two filters and a heater were attached to the water tank to remove the corrosion products and to achieve a faster and more consistent corrosion rate (Fig. 6). The steel specimen surface showed the expected unevenness and roughness typical for the corrosion process.

The high frequency guided waves (superposition of fundamental A_0 and S_0 Lamb modes) were generated at the upper plate surface using a standard Rayleigh angle beam transducer with a center frequency of 0.5 MHz. As for the FE simulations, the excitation signal was chosen as a narrowband 10-cycle tone burst, generated in a programmable function generator and amplified using a broadband power amplifier. A heterodyne laser vibrometer was used for point measurements of the out-of-plane velocity component of the steel plate surface along the center line of propagation [28], as shown in Fig. 7. The laser head was fixed to a scanning rig and moved parallel to the plate surface with a step size of 1 mm for a distance of 450 mm from the front of the transducer wedge. The laser vibrometer signal was filtered using a bandpass filter (0.4-0.6 MHz), averaged (50 averages) and recorded using a digital storage oscilloscope before being transferred to a computer. The same evaluation and fitting procedure as for the FE simulations was performed using Matlab. For each plate thickness the wave field amplitude was extracted at 0.45 MHz (FFT) along the center line of the specimen and displayed versus propagation distance.

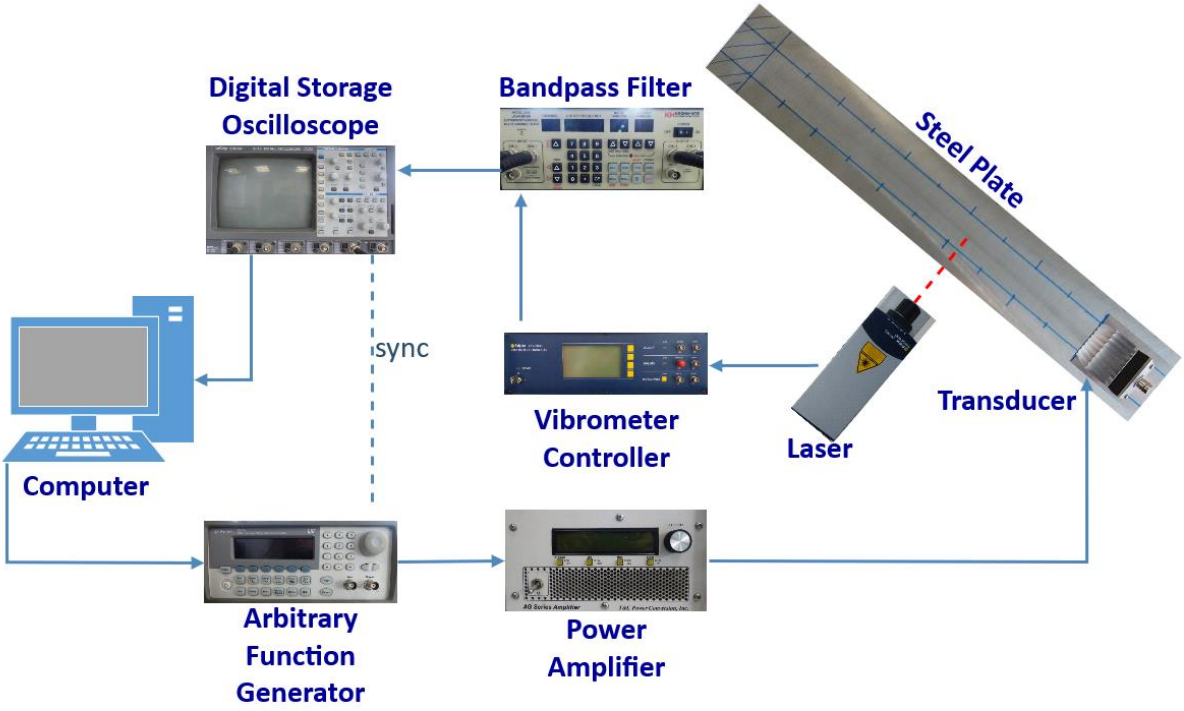

Figure 7. Schematic of experimental setup for laser measurement of high frequency guided wave propagation on steel specimen.

5. Experimental Results

5.1. Milled Specimen with uniform thickness reduction

The first plate specimen was milled in approximately 0.2 mm steps from a uniform thickness of 11.0 mm to 9.43 mm. The amplitude variation due to the beating effect between the two fundamental guided wave modes can be clearly observed in Fig. 8. The amplitude on the top plate surface at 0.45 MHz (FFT) decreases as the wave propagates from the excitation wedge location and then periodically increases and decreases again due to the interference caused by the slightly different phase velocities. The experimental curves do not go to zero amplitude due to slightly different effective excitation amplitudes for the A_0 and S_0 modes.

The amplitude variation over shorter length scales is mostly due to an interference with higher wave modes (especially the A_1 mode). The measured amplitude curves were fitted with the theoretically predicted exponentially decreasing cosine curve using Matlab. Good agreement for the principal features can be seen in Fig. 8 for the measurements at different plate thicknesses. As predicted from the FE simulation results, the beatlength decreases with decreasing plate thickness and amplitude minima and maxima occur over a shorter length scale. For the thicker plates, the longer beatlength leads to only one amplitude minimum and maximum over the measurement length and the fitting procedure to determine the beatlength was found to be less accurate than for measurements on thinner plates, where multiple minima and maxima occur. Beatlengths were evaluated for each of the 9 available milled, uniform plate thicknesses and are compared and discussed in section 5.3.

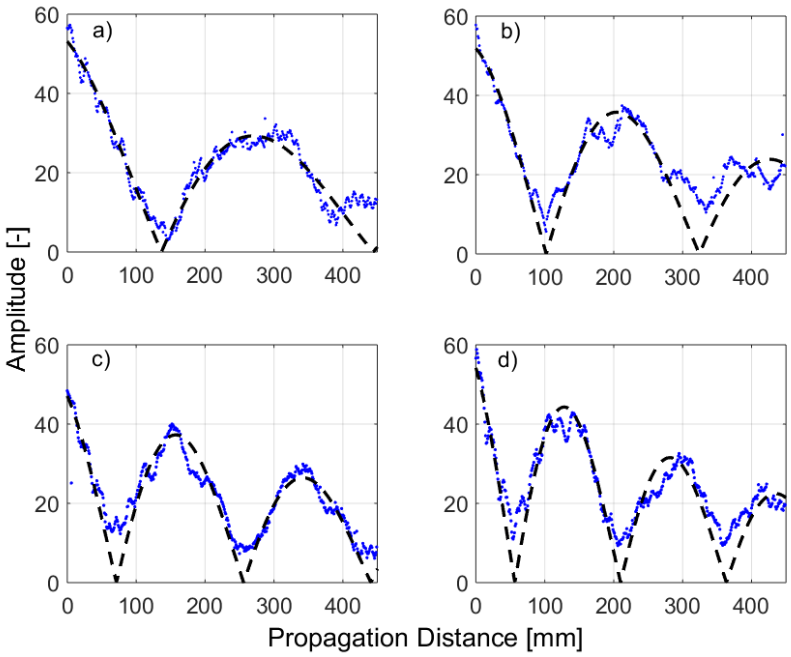

Figure 8. Amplitude of high frequency guided wave at 0.45 MHz (FFT) along milled steel specimen: (a) 11.00 mm; (b) 10.39 mm; (c) 9.80 mm, (d) 9.43 mm thickness; measured amplitude: blue dots; exponential fit: black dashed line.

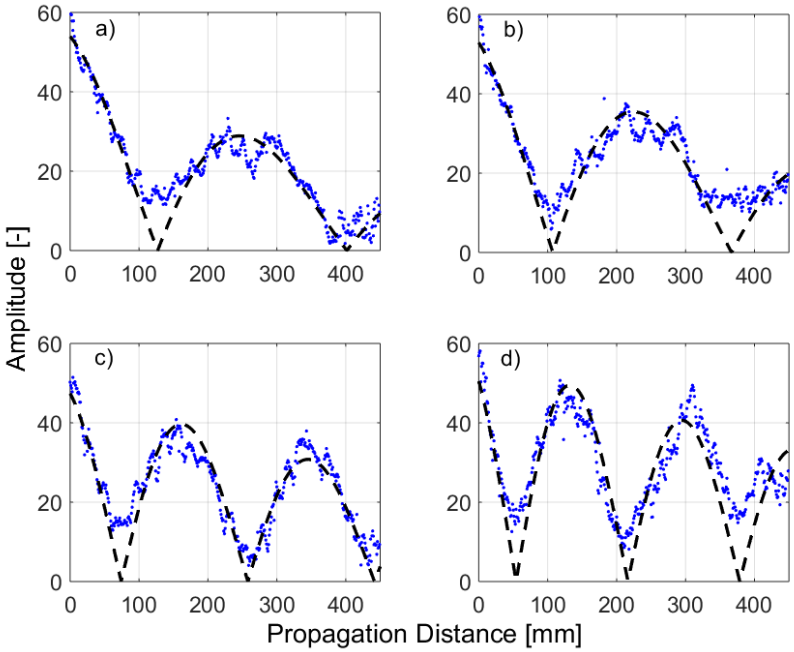

Figure 9. Amplitude of high frequency guided wave at 0.45 MHz (FFT) along corroded steel specimen #A: a) 10.80 mm; b) 10.49 mm, c) 9.82 mm, d) 9.42 mm approximate thickness; measured amplitude: blue dots; exponential fit: black dashed line.

5.2. Corroded specimens

The accelerated corrosion of the two plate specimens was interrupted regularly to achieve plate thickness reductions of approximately 0.2 mm for the measurement of the guided wave propagation. Similar behavior with periodic amplitude increase and decrease due to the wave interference is shown in Fig. 9 for one of the specimens. The experimental amplitude variation for the corroded plate specimens is similar to the one obtained for the milled specimen. No significant difference due to the unevenness and roughness of the corroded surface was observed. The maximum measured thickness variation of up to approximately 0.3 mm was gradual and corrosion pitting or steep thickness changes that might lead to wave scattering were not observed. The fit of the exponentially decreasing cosine curve matches the amplitude measurements on the corroded plate quite well, and the decrease in beatlength with decreasing thickness can be clearly observed. The beatlength was evaluated at respectively 7 and 5 thickness values for the two corroded specimens with final thickness of 9.42 mm, respectively 9.84 mm.

5.3. Beatlength evaluation

Figure 10 shows the evaluation of the beatlength at 0.45 MHz (FFT, fit) for the experiments on the milled and corroded steel plates against the plate thickness (actual measured values). Reasonably good agreement with the theoretically predicted beatlength can be observed for the decrease in beatlength with plate thickness.

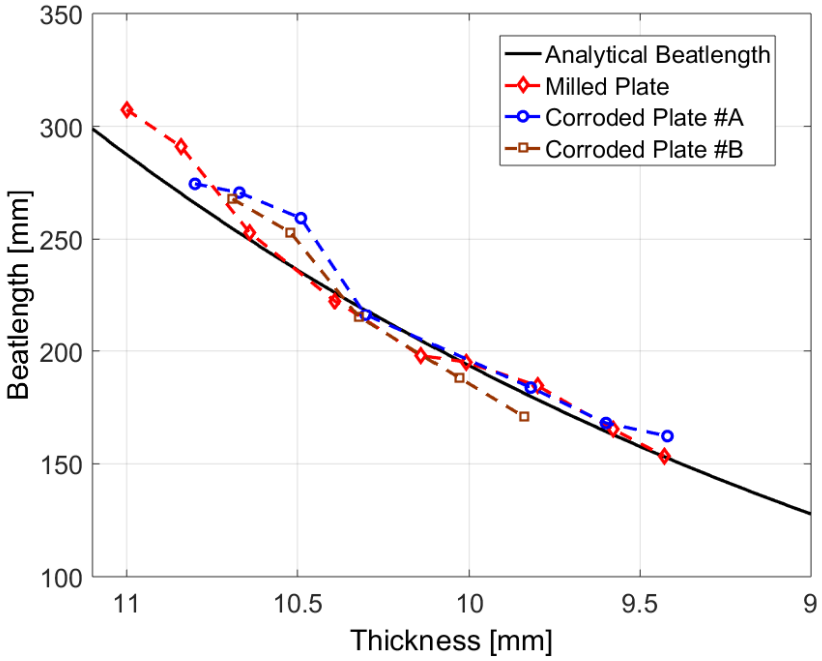

Figure 10. Comparison of theoretically predicted beatlength at 0.45 MHz (solid, black line) against measured beatlength (fit from laser amplitude measurements at 0.45 MHz); milled specimen: red diamonds; corroded specimens: blue circles (specimen #A), brown squares (specimen #B).

For the thicker steel plates, the measurement length of 450 mm was comparable with the beatlength with only one minimum and maximum visible, resulting in a larger uncertainty in the beatlength value obtained from the fitting procedure. This error decreases with reduced beatlength and overall a good match and significant changes in beatlength can be observed. For the milled plate, the experimental beatlength has a maximum error of less than 8% for all measurements, with an error below 4% for plate thicknesses below 10.8 mm. The maximum error in the evaluated beatlength for the corroded steel plates was slightly larger than for the milled, uniform thickness reduction, with a maximum error of approximately 10%. This might be partially due to the roughness and thickness variation along the specimen length due to corrosion, where the average thickness was found to match well with observed changes in beatlength. More significant thickness variation or pitting corrosion might lead to additional guided wave scattering and complicate beatlength measurements.

For the overall change in thickness of about 1.6 mm (14% relative thickness reduction), the beatlength changes by approximately 45% for both the milled and corroded specimens, in line with theoretical predictions. This demonstrates the sensitivity of the beatlength to the thickness due to it being dependent on the inverse of the wave number difference between the fundamental modes. Therefore, small changes in plate thickness cause relatively large variation of the beatlength, which can be measured accurately. Taking into account the experimental errors for the determination of the plate thickness reduction, the beatlength evaluation is sensitive enough to obtain a resolution of approximately 0.3 mm (3% of plate thickness), which would be more than sufficient to detect and monitor generalized corrosion wall thickness loss before it affects the structural integrity of marine structures such as ship hulls or offshore oil and gas installations.

6. Conclusions

Wall thickness loss due to the corrosive environment is a significant problem for a range of engineering applications, including pipelines and marine structures. The monitoring of wall thickness reduction was investigated employing the interference of high frequency guided waves propagating along the structure. This allows for the measurement over a reasonable propagation length along the specimen as compared to through-thickness ultrasonic point by point measurements. The measurement principle and evaluation were simulated using 2D FE modelling and the expected guided wave propagation and mode interference visualized. The high frequency guided wave modes (fundamental A_0 and S_0 Lamb modes) at approximately 5 MHz mm frequency thickness product (0.5 MHz, 9-11 mm thick steel plate) were excited selectively using a standard ultrasonic wedge transducer and the wave propagation along the steel plates of different thicknesses measured using a laser interferometer. The interference pattern over a length scale called the beatlength depends on the inverse of the difference in the respective wavenumbers and is very sensitive to changes in the plate thickness.

One plate specimen was milled down in successive steps to achieve uniform plate thickness reduction. The wall thickness of two mild steel plates was reduced using accelerated corrosion, resulting in the typical unevenness and roughness of the plate surface due to the corrosion process. The guided wave beatlength was quantified from a fit of the experimentally measured amplitude curves along the propagation distance for the different plate thicknesses and good agreement of the measured beatlengths with theoretical predictions was achieved. The proposed methodology has good sensitivity with a significant reduction in beatlength with thickness. From the experimental results, the sensitivity for wall thickness loss was estimated at about 3% under laboratory conditions, sufficient to detect and monitor generalized corrosion before it affects the structural integrity, e.g., of ship hulls or offshore installations.

Acknowledgements

The authors would like to thank Jason Sanderson and Adrian Safciuc for their contribution to the development of the guided ultrasonic wave and corrosion measurement procedures, and Fabian Bernhard for the theoretical contributions.

References

[1] S. Sharma, A. Mukherjee, “Ultrasonic guided waves for monitoring corrosion in submerged plates,” *Struct. Control Health Monit.* 22, 19–35 (2015).
[2] T. Nakai, H. Matsushita, N. Yamamoto, H. Arai, “Effect of pitting corrosion on local strength of hold frames of bulk carriers (1st report),” *Marine Struct.* 17, 403-432 (2004).
[3] P. Cawley, F. Cegla, M. Stone, “Corrosion Monitoring Strategies - Choice Between Area and Point Measurements,” *J. Nondestruct. Eval.* 32, 156-163 (2013).
[4] J.S. Hall, P. Fromme, J.E. Michaels, “Guided Wave Damage Characterization via Minimum Variance Imaging with a Distributed Array of Ultrasonic Sensors,” *J. Nondestruct. Eval.* 33, 299-308 (2014).
[5] J. L. Rose, “Standing on the shoulders of giants: An example of guided wave inspection,” *Mat. Eval.* 60, 53-59 (2002).
[6] L. Zeng, Z. Luo, J. Lin, J. Hua, “Excitation of Lamb waves over a large frequency-thickness product range for corrosion detection,” *Smart Mater. Struct.* 26, 095012 (2017).

[7] P. Fromme, P.D. Wilcox, M.J.S. Lowe, P. Cawley, "On the development and testing of a guided ultrasonic wave array for structural integrity monitoring," *IEEE Trans. Ultrason. Ferroelectr. Freq. Control* 53, 777-785 (2006).
[8] J. Wang, Y. Shen, "An enhanced Lamb wave virtual time reversal technique for damage detection with transducer transfer function compensation", *Smart Mater. Struct.* 28, 085017 (2019).
[9] F. Jenot, M. Ouaftouh, M. Duquennoy, M Ourak, "Corrosion thickness gauging in plates using Lamb wave group velocity measurements," *Meas. Sci. Technol.* 12, 1287–1293 (2001).
[10] P. Huthwaite, R. Ribichini, P. Cawley, M.J.S. Lowe, "Mode Selection for Corrosion Detection in Pipes and Vessels via Guided Wave Tomography," *IEEE Trans. Ultrason. Ferroelectr. Freq. Control* 60, 1165-1177 (2013).
[11] P.B. Nagy, F. Simonetti, G. Instanes, "Corrosion and erosion monitoring in plates and pipes using constant group velocity Lamb wave inspection", *Ultrasonics* 54, 1832-1841 (2014).
[12] R. Howard, F. Cegla, "On the probability of detecting wall thinning defects with dispersive circumferential guided waves," *NDT & E Int.* 86, 73-82 (2017).
[13] P. Khalili, P. Cawley, "The choice of ultrasonic inspection method for the detection of corrosion at inaccessible locations," *NDT & E Int.* 99, 80-92 (2018).
[14] S.F. Burch, N.J. Collett, S. Terpstra, M.V. Hoekstra, "M-skip: A quantitative technique for the measurement of wall loss in inaccessible components," *Insight* 49, 190-194 (2007).
[15] D.W. Greve, P. Zheng, I.J. Oppenheim, "The transition from Lamb waves to longitudinal waves in plates," *Smart Mater. Struct.* 17, 035029 (2008).
[16] N. Terrien, D. Osmont, D. Royer, F. Lepoutre, A. Déom, "A combined finite element and modal decomposition method to study the interaction of Lamb modes with micro-defects," *Ultrasonics* 46, 47-78 (2007).
[17] D. Ratnam, K. Balasubramaniam, B.W. Maxfield, "Generation and Detection of Higher-Order Mode Clusters of Guided Waves (HOMC-GW) Using Meander-Coil EMATs," *IEEE Trans. Ultrason. Ferroelectr. Freq. Control* 59, 727-737 (2012).
[18] B. Masserey, P. Fromme, "In-Situ Monitoring of Fatigue Crack Growth using High Frequency Guided Waves," *NDT&E Int.* 71, 1-7 (2015).
[19] B. Masserey, P. Fromme, "Surface defect detection in stiffened plate structures using Rayleigh-like wave," *NDT & E Int.* 42, 564-572 (2009).
[20] D. Chew, P. Fromme, "Monitoring of corrosion damage using high-frequency guided ultrasonic waves," *Proc. SPIE* 9064, 90642F (2014).
[21] D. Chew, P. Fromme, "High-frequency Guided Waves for Corrosion Monitoring," *AIP Conf. Proc.* 1650, 777-784 (2015).
[22] J. Virieux, "P-SV wave propagation in heterogeneous media: Velocity-stress finite-difference method," *Geophysics* 51, 889–901 (1986).
[23] B. Masserey, E. Mazza, "Analysis of the near-field ultrasonic scattering at a surface crack," *J. Acoust. Soc. Am.* 118, 3585–3594 (2005).
[24] B. Masserey, C. Raemy, P. Fromme, "High-frequency guided ultrasonic waves for hidden defect detection in multi-layered aircraft structures," *Ultrasonics* 54, 1720-1728 (2014)
[25] B. W. Ti, W. D. O'Brien, J. G.Harris, "Measurements of coupled Rayleigh wave propagation in an elastic plate," *J. Acoust. Soc. Am.* 102, 1528-1531 (1997).
[26] B.A. Auld, "*Acoustic Fields and Waves in Solids*," New York, Wiley, 1973, Vol. 2.
[27] B. Pavlakovic, M.J.S. Lowe, D. Alleyne, P. Cawley, "Disperse: general purpose program for creating dispersion curves," *Rev. Prog. QNDE* 16, Plenum Press, 185-192 (1997).
[28] B. Masserey, P. Fromme, "High-frequency guided waves for defect detection in stiffened plate structures," *Insight* 51, 667-671 (2009).